Fabrication and characterization of electrospun titania nanofibers

Ramya Chandrasekar · Lifeng Zhang · Jane Y. Howe · Nyle E. Hedin · Yan Zhang · Hao Fong

Abstract Titania (TiO$_2$) nanofibers were fabricated by electrospinning three representative spin dopes made of titanium (IV) *n*-butoxide (TNBT) and polyvinylpyrrolidone (PVP) with the TNBT/PVP mass ratio being 1/2 in three solvent systems including *N,N*-dimethylformamide (DMF), isopropanol, and DMF/isopropanol (1/1 mass ratio) mixture, followed by pyrolysis at 500 °C. The detailed morphological and structural properties of both the as-electrospun precursor nanofibers and the resulting final TiO$_2$ nanofibers were characterized by SEM, TEM, and XRD. The results indicated that the precursor nanofibers and the final TiO$_2$ nanofibers made from the spin dopes containing DMF alone or DMF/isopropanol mixture as the solvent had the common cylindrical morphology with diameters ranging from tens to hundreds of nanometers, while those made from the spin dope containing isopropanol alone as the solvent had an abnormal concave morphology with sizes/widths ranging from sub-microns to microns. Despite the morphological discrepancies, all precursor nanofibers were structurally amorphous without distinguishable phase separation, while all final TiO$_2$ nanofibers consisted of anatase-phased TiO$_2$ single-crystalline grains with sizes of approximately 10 nm. The electrospun TiO$_2$ nanofiber mat is expected to significantly outperform other forms (such as powder and film) of TiO$_2$ for the solar cell (particularly dye-sensitized solar cell) and photo-catalysis applications.

R. Chandrasekar · L. Zhang · N. E. Hedin · H. Fong (✉)
Department of Chemistry, South Dakota School of Mines and Technology, Rapid City, SD 57701, USA
e-mail: hao.fong@sdsmt.edu

J. Y. Howe
Materials Science and Technology Division, Oak Ridge National Laboratory, Oak Ridge, TN 37831, USA

Y. Zhang (✉)
School of Physics and Materials Science, Anhui University, Hefei, Anhui 230039, China
e-mail: zhangyaner2005@163.com

Introduction

Titania is a wide band-gap semi-conductive ceramic with many important applications including, but not limited to, solar cell and photo-catalysis [1–5]. Titania has two common crystalline forms: the rutile and the anatase form. Although both are expressed using the same chemical formula of TiO$_2$, the rutile TiO$_2$ has a tetragonal crystalline structure, while the anatase TiO$_2$ has an octahedral crystalline structure. For the solar cell and photo-catalysis applications, only the anatase TiO$_2$ exhibits high activities. The band-gap value for the anatase TiO$_2$ is 3.2 eV, which is equivalent to the energy of sunlight with the wavelength of 388 nm. The anatase TiO$_2$ can absorb energy either directly from the sunlight or indirectly from light-sensitizers such as dyes, causing electrons to excite and/or jump to the conduction band and create positive holes in the valence band. This is termed as charge separation in solar cells, and the separated charges can be converted into electricity [1–3]. Additionally, the excited electrons possess a reduction capability, while the positive holes possess an oxidation capability; and the anatase TiO$_2$ has therefore been applied in the remediation of a variety of organic compounds and heavy metal ions (such as Pt^{4+}, Pd^{2+}, and Cr^{3+}) from aqueous solutions as well as the destruction of microorganisms such as bacteria, viruses, and molds [4, 5]. The photo-voltaic performance and photo-catalytic efficiency of the anatase TiO$_2$ are strongly influenced by the specific surface area as well as the overall morphology.

The electrospun TiO_2 nanofiber mat with nanofibers randomly overlaid, having diameters ranging from tens to hundreds of nanometers, and consisting of anatase-phased TiO_2 single-crystalline grains with sizes of approximately 10 nm, is expected to significantly outperform other forms (such as powder and film) of TiO_2 for solar cell and photo-catalysis applications. This is because the electrospun TiO_2 nanofiber mat has a high specific surface area (ranging from hundreds to thousands of square meters per gram) and controllable pore sizes among the nanofibers (ranging from tens to hundreds of nanometers); additionally, the thickness of the mat can be readily manipulated. Unlike nanoscaled TiO_2 particles/rods which are in loose granular form, the electrospun TiO_2 nanofibers are well contained within the mat/felt. For the solar cell (particularly the dye-sensitized solar cell) application, the electrospun TiO_2 nanofiber mat can provide a continuous transporting pathway for the photo-generated electrons and result in high performance/efficiency. Presently, most dye-sensitized solar cells are made from powders consisting of TiO_2 nanoparticles and the photo-generated electrons move via hopping through the nanoparticles. It is well-known that hopping is not an efficient pathway for electron transportation, and the electron loss/recombination is high during hopping [1–3]. For the photo-catalysis application, the large specific surface area of the electrospun TiO_2 nanofiber mat leads to a large number of reaction sites which enhances the catalytic efficiency/activity; additionally, the nanofiber mat morphology also provides a great accessibility for reactants during the application [4, 5].

Electrospinning is a technique that utilizes electric forces alone to drive the spinning process and to produce fibers. Unlike conventional spinning techniques such as solution spinning and melt spinning that are capable of producing fibers with diameters in the micrometer range ($\sim$5–15 μm), electrospinning is capable of producing fibers with diameters in the nanometer range ($\sim$50–1,000 nm). Unlike nanotubes, nanowires, and nanorods, most of which are made by bottom-up methods and usually require further expensive purifications, electrospun nanofibers are made through a top-down nanomanufacturing process. Electrospun nanofibers are therefore inexpensive, continuous, and also relatively easy to align, assemble, and process into applications. In the recent decade, the technique of "electrospinning" and its unique product of "nanofibers" have been actively researched throughout the world [6–15].

Electrospun ceramic nanofibers are made by electrospinning spin dopes containing precursors of ceramics followed by high temperature pyrolysis. Numerous electrospun ceramic nanofibers, including silica (SiO_2) and titania (TiO_2) nanofibers, have been fabricated and studied [16–21]. Electrospun TiO_2 nanofibers have been studied with particular interest because of well-studied precursors and wide applications. In recent years, a variety of spin dopes have been investigated. The spin dopes can be generally classified into two types including: (1) sol–gels made from alkoxide precursors such as titanium (IV) *n*-butoxide (TNBT), and (2) organic solutions containing alkoxide precursors and carrying polymers such as polyvinylpyrrolidone (PVP). The pH value and concentration of the sol–gel type of spin dopes have to be judiciously adjusted to precisely control the gelation extent of alkoxide precursors and the related spin dope viscosity. If the spin dope viscosity is too low, the as-electrospun nanofibers will contain beads and/or beaded nanofibers [22]. If the spin dope viscosity is too high, electrospinning will not be stable or cannot even be conducted. On the other hand, viscosity and other properties of the organic solution type of spin dopes are much more convenient to adjust and control; and the as-electrospun nanofibers are generally more uniform with fewer beads and/or beaded nanofibers [17, 23]. Therefore, this type of spin dopes is more widely adopted. No matter which type of spin dopes is used for electrospinning, the as-electrospun precursor nanofibers (after being placed under the ambient conditions for a period of time to allow the moisture in air to completely hydrolyze/gel the alkoxide precursors) must undergo a high temperature pyrolysis process to burn/remove the organic components for the fabrication of the final TiO_2 nanofibers. Many reported research efforts have been focused on the potential applications of electrospun TiO_2 nanofibers [18–21], whereas few systematic investigations have been carried out on: (1) the optimization of spin dope properties and electrospinning conditions, and (2) the detailed characterization of morphological and structural properties of electrospun TiO_2 nanofibers.

The objective of this study was to systematically investigate the fabrication and characterization of electrospun TiO_2 nanofibers for the future research on solar cell (particularly dye-sensitized solar cell) and photo-catalysis applications. The study was primarily focused on the detailed examination of morphological and structural properties of both the as-electrospun precursor nanofibers and the resulting final TiO_2 nanofibers made from three representative spin dope systems.

Experimental

Materials

Titanium (IV) *n*-butoxide (TNBT, catalog number 244112), polyvinylpyrrolidone (PVP, catalog number 437190, $M_w = 1,300,000$), *N,N*-dimethylformamide (DMF, catalog number 227056, anhydrous), isopropanol (catalog number

278475, anhydrous), and acetic acid (HAc, catalog number 537020, glacial) were purchased from the Sigma-Aldrich Co. (Milwaukee, Wisconsin) and used without further purification.

Spin dopes

Many organic solution type of spin dopes were prepared and studied in this research. The spin dopes had various concentrations of TNBT and PVP, and the solvent systems were different combinations of DMF and isopropanol with a trace amount (∼2 wt.%) of HAc. HAc was added in the spin dopes to control the hydrolysis/gelation of TNBT. In general, (1) if the concentration of PVP was too low, the as-electrospun nanofibers would have beads and/or beaded nanofibers; if the concentration was too high, the diameters of as-electrospun nanofibers would be large [17]; and (2) if the mass ratio of TNBT/PVP was too low, the yield/productivity of the final TiO_2 nanofibers would be low and the nanofibers would tend to break; if the mass ratio was too high, the as-electrospun nanofibers would tend to stick together [17]. The following three spin dopes were identified as the optimal and representative systems.

A. 6 wt.% TNBT and 12 wt.% PVP in DMF.
B. 4 wt.% TNBT and 8 wt.% PVP in DMF/isopropanol mixture with the mass ratio of 1/1.
C. 2 wt.% TNBT and 4 wt.% PVP in isopropanol.

Electrospinning

A specially designed bullet-shaped spinneret was used to conduct the electrospinning, and the electrospinning was conducted in an open environment at the room temperature of approximately 25 °C. The spinneret consisted of a high-density polypropylene tube with an inner diameter of 1.0 inches and a stainless steel hemispherical head with an orifice having a diameter of 0.5 mm at the center. The electrospinning setup included a high voltage power supply (ES30P) purchased from the Gamma High Voltage Research, Inc. (Ormond Beach, Florida) and a laboratory-built roller with diameter of 10 inches. During electrospinning, a positive high voltage of 15 kV was applied through a thin stainless steel rod to the spin dope held inside the spinneret. As-electrospun nanofibers were collected on the electrically grounded aluminum foil that covered the roller. The rotational speed of the roller was set at 100 rpm during electrospinning. This process of electrospinning was extremely stable, and the electrospinning jet ran continuously without breaking for several hours. The mat collected on the aluminum foil was, hypothetically, a single nanofiber loosely aligned along the rotational direction. A heat lamp was used to dry the nanofiber mat during electrospinning, and the as-electrospun TNBT/PVP precursor nanofiber mat was kept at 25 °C in an open environment with the relative humidity of approximately 50% for 24 h to allow the TNBT in the nanofibers to completely hydrolyze and turn into a three dimensional network (gel).

Pyrolysis

The precursor nanofibers were carefully peeled off from the aluminum foil, transferred into a ceramic boat, and placed in a Lindberg 54453 Heavy Duty Tube Furnace purchased from the TPS Co. (Watertown, Wisconsin) for pyrolysis into the final TiO_2 nanofibers. The procedure for pyrolysis included: (1) increasing the temperature at the 10 °C per minute rate from the room temperature to 500 °C, (2) maintaining the temperature at 500 °C for 6 h to completely burn/remove the organic components in the fibers and to allow TiO_2 to crystallize, and (3) naturally cooling off to room temperature. A constant flow of air was maintained through the furnace during the pyrolysis.

Characterizations

A Zeiss Supra 40VP field-emission SEM and a Rigaku Ultima Plus XRD at the South Dakota School of Mines and Technology, as well as a Hitachi HF-3300 TEM/STEM at the Oak Ridge National Laboratory, were employed to characterize the morphological and structural properties of both the as-electrospun precursor nanofibers and the resulting final TiO_2 nanofibers. Prior to SEM examination, the specimens were sputter-coated with gold to avoid charge accumulations. A rotating X-ray generator (40 kW, 40 mA) with $CuK\alpha$ radiation (wavelength $\lambda = 1.54$Å) was used during the XRD experiments. The XRD profiles were recorded from 10 to 70° at the scanning speed of $2°$ min^{-1}. For the high-resolution TEM characterizations, an acceleration voltage of 100 kV was selected for the precursor nanofibers and an acceleration voltage of 300 kV was selected for the final TiO_2 nanofibers. The TEM specimens were prepared by dispersing fibers onto lacey carbon films supported on 200-mesh copper grids.

Results and discussion

TNBT has been extensively studied as the alkoxide precursor for making TiO_2, and was thus selected in this research. PVP has been reported for fabrication of electrospun ceramic nanofibers in several publications [17, 19–21], and was thus selected as the carrying polymer. PVP is soluble in many solvents (such as water, isopropanol, DMF, and their mixtures) and has low toxicity;

additionally, the thermal behavior of PVP also makes it suitable as a carrying polymer since PVP decomposes before melting starts, therefore the fiber morphology can be well-retained during pyrolysis. Isopropanol was selected because it is a good solvent for both TNBT and PVP eventhough it is not a good electrospinning solvent due to its high volatility and low dielectric constant [14]. DMF was selected because it is a well-known good solvent for electrospinning due to its high dielectric constant and appropriate volatility [14, 17]. However, TNBT is not highly soluble in DMF. As shown in Fig. 1, the spin dope "A" made of DMF alone as the solvent was a milky but uniform emulsion because PVP acted as the emulsifier to stabilize the tiny droplets of TNBT in DMF; both the spin dope "B" made of DMF/isopropanol mixture as the solvent and the spin dope "C" made of isopropanol alone as the solvent were clear solutions.

The SEM images in Fig. 2 showed the representative morphologies of the as-electrospun precursor nanofibers made from the spin dopes "A", "B", and "C", respectively. The TNBT/PVP mass ratio of 1/2 was maintained as the same in the three samples. Almost no beads and/or beaded fibers were identified within the scope of this investigation. The fibers made from the spin dopes containing DMF alone ("A") or DMF/isopropanol mixture ("B") as the solvent had a common cylindrical morphology with diameters ranging from ~50 to ~500 nm, whereas those made from the spin dope containing isopropanol alone ("C") as the solvent had an abnormal concave morphology with sizes/widths ranging from ~200 nm to ~2 μm. The dielectric constant of isopropanol is 19.9, while that of DMF is 39. The relatively low dielectric constant of isopropanol made the electrospinning jet of spin dope "C" carry a relatively small amount of excess charges, thus reducing the stretching during electrospinning and resulting in the formation of fibers with relatively large sizes. The concave morphology was
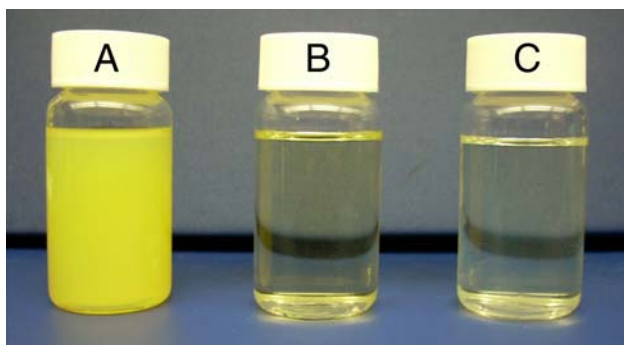
Fig. 1 Photo images of the spin dope "A" made of TNBT, PVP, and DMF; the spin dope "B" made of TNBT, PVP, and DMF/isopropanol (1/1 mass ratio) mixture; and the spin dope "C" made of TNBT, PVP, and isopropanol
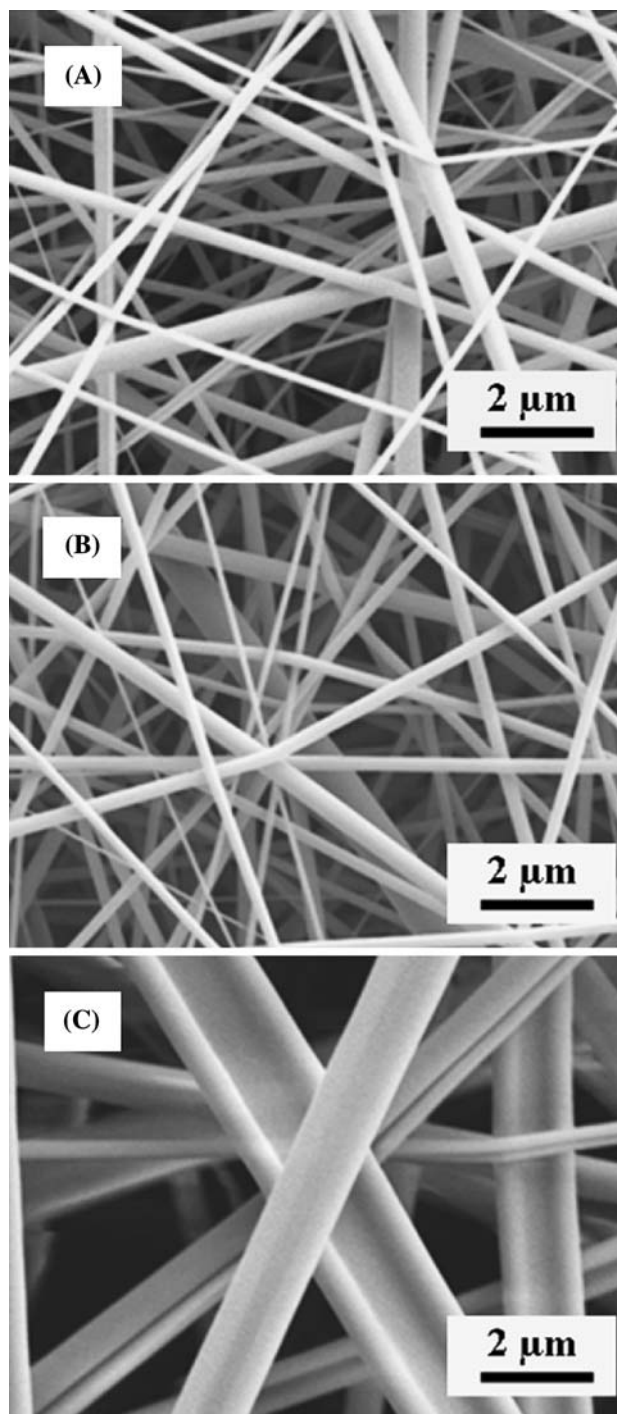
Fig. 2 Representative SEM images of the precursor nanofibers made from the spin dopes "A", "B", and "C", respectively

presumably caused by the formation and collapse of hollow jets/fibers [24]. During electrospinning, the traveling jets solidify into fibers through solvent evaporation; therefore the solvent volatility plays an important role in fiber formation. Isopropanol has a high volatility and this could cause the surface of an electrospinning jet to be solidified while the inside is not. Such a condition would lead to the

formation of hollow jets/fibers; and the collapse of these hollow jets/fibers would result in the formation of the concave morphology. Intriguingly, the morphologies of the fibers made from spin dopes "A" and "B" were nearly identical. This suggested that the fiber formation from the spin dope "B" occurred after isopropanol had almost completely evaporated/removed from the electrospinning jet; in other words, the solidification occurred when there was merely DMF left as the solvent in the electrospinning jet.

Figure 3 showed the representative TEM images of the precursor nanofibers made from the spin dopes "A", "B", and "C", respectively. Consistent with the SEM observations, the fibers had different diameters/sizes and morphologies. The two particular nanofibers as shown in Fig. 3a and b had diameters of approximately 100 nm, which were relatively thin among the nanofibers made from the spin dopes "A" and "B", respectively. The particular fiber as shown in Fig. 3c had a size/width of approximately 800 nm, which was also relatively thin among the nanofibers made from the spin dope "C"; the TEM image also indicated that this fiber had a concave morphology since the center of the fiber was apparently thinner than the edge. Intriguingly, the three precursor nanofibers were all structurally uniform without any identifiable phase separation, despite that the spin dope "A" was an emulsion while the spin dopes "B" and "C" were solutions; furthermore, the diffraction patterns (the insets in Fig. 3) indicated that all three precursor nanofibers were structurally amorphous. The following are our proposed explanations. During electrospinning, when the electrostatic field reaches a critical value and the electric force overcomes the surface tension and the viscoelastic force, a jet ejects and travels straight for a certain distance. The jet then starts to bend, forming helical loops. This phenomenon is termed as "bending instability" [7]. Typically, bending instability causes the length of an electrospinning jet to elongate up to 50,000 times in a very short time period (50 ms or less). Thus, the rate of elongation (draw) during bending instability is extremely large (up to $1,000,000 \text{ s}^{-1}$). Such a huge draw rate and the associated extremely intensive stretching and/or shearing could result in the meta-stable and almost molecularly-uniform mixing of TNBT, PVP, and the solvent, no matter the solvent is DMF, isopropanol, or DMF/isopropanol mixture. Additionally, the solvent evaporation rate during electrospinning, particularly during bending instability, is extremely fast (i.e., over 99% solvent is removed/evaporated from the jet in less than 0.1 s [17]). Therefore, the molecular mixing of TNBT and PVP can be maintained in the as-electrospun precursor nanofibers.

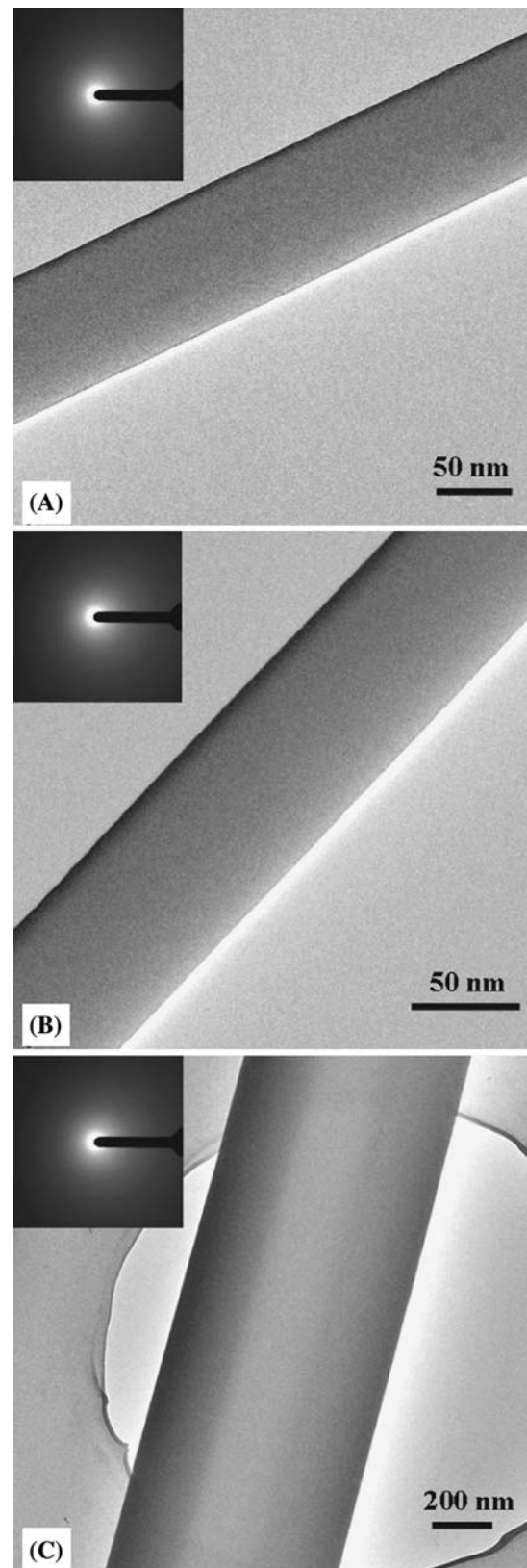The SEM images in Fig. 4 showed the representative morphologies of the final electrospun TiO₂ nanofibers

Fig. 3 Representative TEM images and electron diffraction patterns (insets) of the precursor nanofibers made from the spin dopes "A", "B", and "C", respectively
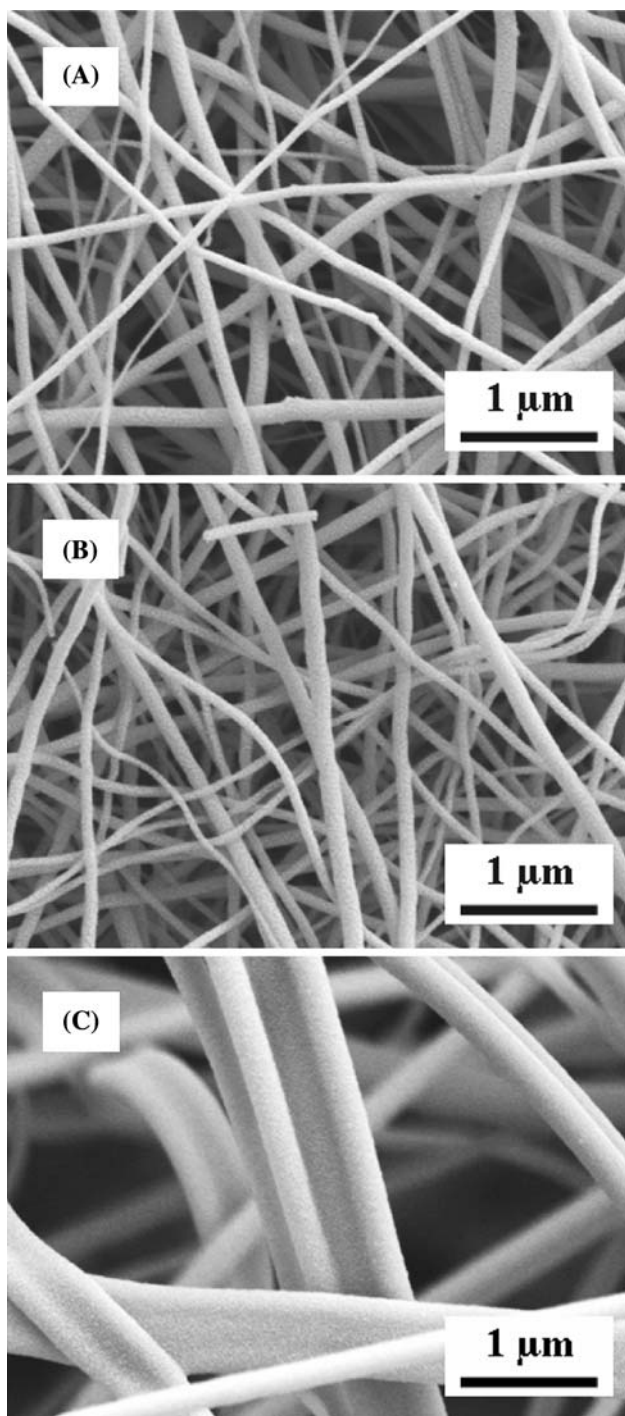
Fig. 4 Representative SEM images of the electrospun TiO$_2$ nanofibers made from the spin dopes "A", "B", and "C", respectively

made from the spin dopes "A", "B" and "C", respectively. In our early experiments, the pyrolysis temperature was set at 450 °C, because we had a concern that a higher temperature (usually 550 °C or higher) would result in the formation of the rutile-phased TiO$_2$; we found that the prepared TiO$_2$ nanofibers often contained trace amount of a black solid (presumably carbon), and the solid remained

even after pyrolysis at 450 °C for several days. This indicated that the PVP was not completely burnt/removed and the pyrolysis temperature of 450 °C might be too low. The thermogravimetric analysis (TGA) was then carried out on the precursor nanofibers; and the results suggested that a minimum temperature of 500 °C was required to completely burn/remove PVP in the precursor nanofibers in air (TGA curves not shown). Thus, 500 °C was adopted as the pyrolysis temperature. As shown in Fig. 4, the three final TiO$_2$ nanofibers were all significantly thinner than the respective precursor nanofibers; the diameters were 200 nm or less for the ones made from the spin dopes "A" and "B", and the sizes/widths were 600 nm or less for the ones made from the spin dope "C". The contraction in fiber diameter/size was due to the removal of organic components in the precursor nanofibers; and the contraction was consistent with our theoretical calculations. Additionally, the degree of surface roughness for the final TiO$_2$ nanofibers was distinguishably higher than that for the precursor nanofibers; and this was due to the nucleation and growth of anatase-phased TiO$_2$ single-crystalline grains during pyrolysis (see the following paragraph for more discussions).

Figure 5 showed the representative TEM images of the final electrospun TiO$_2$ nanofibers made from the spin dopes "A", "B", and "C", respectively. Except for the discrepancies in diameters/sizes and morphologies that were also indicated in the SEM observations (Fig. 4), the three TEM images in Fig. 5 showed no evident differences in crystalline morphology/structure. Nonetheless, unlike the as-electrospun precursor nanofibers that were amorphous, the final TiO$_2$ nanofibers were polycrystalline with nano-scaled crystallites (grains) having sizes of approximately 10 nm. The grains were quite uniform in size, and they were randomly distributed in the nanofibers as revealed by the electron diffraction patterns/rings (the insets in Fig. 5). We believed that the grains were formed during the pyrolysis of the precursor nanofibers due to both the homogeneous nucleation and the space confinement of the nanofibers. The diffraction patterns also revealed that the inter-planar spacing of all TiO$_2$ grains were around 0.35 nm, which was the characteristic of the anatase-phased TiO$_2$ and such results were consistent with the XRD patterns as shown in Fig. 6. The XRD patterns were indexed according to the previous publication [25]. As compared to the XRD curve acquired from a commercially available anatase-phased TiO$_2$ powder with particle sizes ranging from sub-microns to microns (Fig. 6d), the XRD curves acquired from the electrospun TiO$_2$ nanofibers (Fig. 6a, b, and c) had much broader peak widths. According to the Scherrer equation [26], this suggested that the average size of the single-crystalline grains in the electrospun TiO$_2$ nanofibers was significantly smaller than that in the commercial anatase-
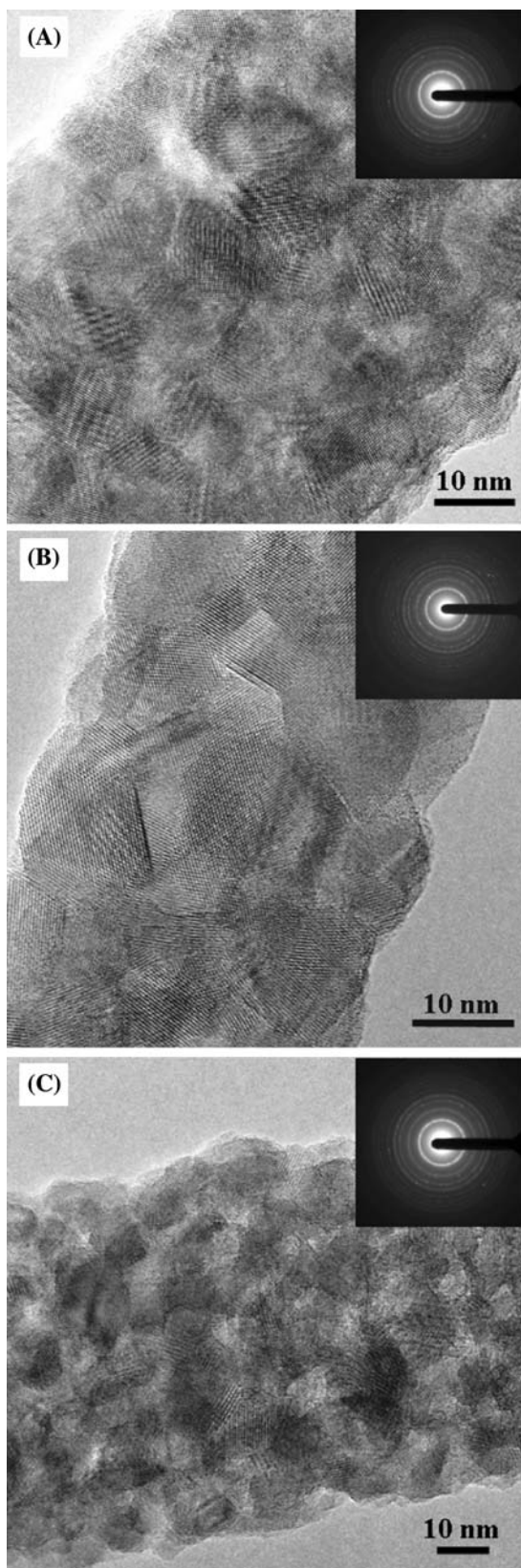
Fig. 5 Representative TEM images and electron diffraction patterns (insets) of the electrospun TiO$_2$ nanofibers made from the spin dopes "A", "B", and "C", respectively
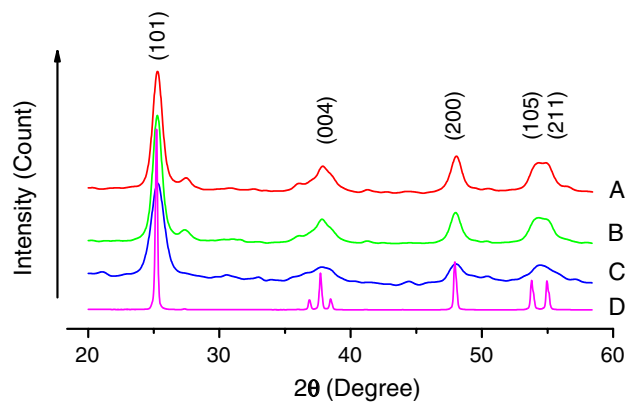

Fig. 6 X-ray diffraction (XRD) patterns of the electrospun TiO$_2$ nanofibers made from the spin dopes "A", "B", and "C", respectively. Curve "D" is the XRD pattern of a commercially available anatase-phased TiO$_2$ powder with the particle sizes ranging from sub-microns to microns

phased TiO$_2$ powder. It is noteworthy that the TEM images were acquired from individual nanofibers while the XRD results were acquired from large amounts of nanofibers in the mats. The consistent results from TEM and XRD confirmed that all electrospun TiO$_2$ nanofibers were made of anatase-phased TiO$_2$ single-crystalline grains with sizes of approximately 10 nm.

Summary

In this study, systematic investigations on the fabrication and characterization of electrospun TiO$_2$ nanofibers were carried out. Three representative spin dopes containing TNBT as the alkoxide precursor and PVP as the carrying polymer (with the TNBT/PVP mass ratio being 1/2) were prepared using DMF, isopropanol, and DMF/isopropanol mixture (with the mass ratio being 1/1) as the solvent, respectively. The spin dopes were electrospun into nanofibers using a laboratory-built setup with a specially designed spinneret; and the nanofibers were collected as overlaid mats. After being placed at 25 °C in an open environment with the relative humidity of approximately 50% for 24 h to allow the hydrolysis/gelation of TNBT to complete, the precursor nanofiber mats were then pyrolyzed at 500 °C to fabricate the final TiO$_2$ nanofibers. The detailed morphological and structural properties of both the precursor nanofibers and the resulting final TiO$_2$ nanofibers were characterized by SEM, TEM, and XRD. The results indicated that the precursor nanofibers and the final TiO$_2$ nanofibers made from the spin dopes containing DMF alone or DMF/isopropanol mixture as the solvent had the common cylindrical morphology with diameters ranging from tens to hundreds of nanometers, while those made

from the spin dope containing isopropanol alone as the solvent had the abnormal concave morphology with sizes/widths ranging from sub-microns to microns. Despite the morphological discrepancies, all precursor nanofibers were structurally amorphous without distinguishable phase separation, whereas all final TiO_2 nanofibers were made of anatase-phased TiO_2 single-crystalline grains with sizes of approximately 10 nm. We envision that the electrospun TiO_2 nanofiber mat would significantly outperform other forms (such as powder and film) of TiO_2 for solar cell (particularly dye-sensitized solar cell) and photo-catalysis applications.

References

1. Yu G, Gao J, Hummelen JC, Wudl F, Heeger AJ (1995) Science 270:1789
2. Bach U, Lupo D, Comte P, Moser JE, Weissorte F, Salbeck J, Spreitzer H, Gratzel M (1998) Nature 395:583
3. Brabec CJ, Sariciftci NS, Hummelen JC (2001) Adv Funct Mater 11(1):15
4. Wold A (1993) Chem Mater 5:280
5. Hoffmann MR, Martin ST, Choi W, Bahnemann DW (1995) Chem Rev 95:69
6. Reneker DH, Chun I (1996) Nanotechnology 7:216
7. Reneker DH, Yarin AL, Fong H, Koombhongse S (2000) J Appl Phys 87:4531
8. Shin YM, Hohman MM, Brenner MP, Rutledge GC (2001) Appl Phys Lett 78:1149
9. Deitzel JM, Kleinmeyer J, Harris D, Beck-Tan NC (2001) Polymer 42:261
10. Bognitzki M, Czado W, Frese T, Schaper A, Hellwig M, Steinhart M, Greiner A, Wendorff JH (2001) Adv Mater 13(1):70
11. Fong H, Reneker DH (2001) In: Salem DR (ed) Structure formation in polymeric fibers. Hanser Gardner, Cincinnati, p 225
12. Huang Z, Zhang Y, Kotaki M, Ramakrishna S (2003) Compos Sci Technol 63:2223
13. Dzenis Y (2004) Science 304:1917
14. Fong H (2007) In: Nalwa HS (ed) Polymeric nanostructures and their applications. American Scientific Publishers, Los Angeles, p 451
15. Greiner A, Wendorff JH (2007) Angew Chem Int Ed 46:5670
16. Choi SS, Lee SG, Im SS, Kim SH, Joo YL (2003) J Mater Sci Lett 22:891
17. Liu Y, Sagi S, Chandrasekar R, Zhang L, Hedin NE, Fong H (2008) J Nanosci Nanotechnol 8:1528
18. Li D, McCann JT, Gratt M, Xia YN (2004) Chem Phys Lett 394:387
19. Li D, Xia YN (2003) Nano Lett 3(4):555
20. Lee SH, Tekmen C, Sigmund WM (2005) Mater Sci Eng A 398:77
21. Nuansing W, Ninmuang S, Jarernboon W, Maensiri S, Seraphin S (2006) Mater Sci Eng B 131:147
22. Fong H, Chun I, Reneker DH (1999) Polymer 40:4585
23. Theron SA, Zussman E, Yarin AL (2004) Polymer 45:2017
24. Arinstein A, Zussman E (2007) Phys Rev E 76:056303
25. Zhang Z, Zhong X, Liu S, Li D, Han M (2005) Angew Chem Int Ed 44:3466
26. Alexander LE (1969) X-ray diffraction methods in polymer science. Wiley, New York